

RNA LOCALIZATION

Global mRNA polarization regulates translation efficiency in the intestinal epithelium

Andreas E. Moor,¹ Matan Golan,¹ Efi E. Massasa,¹ Doron Lemze,¹ Tomer Weizman,¹ Rom Shenhav,¹ Shaked Baydatch,¹ Orel Mizrahi,² Roni Winkler,² Ofra Golani,³ Noam Stern-Ginossar,² Shalev Itzkovitz^{1*}

Asymmetric messenger RNA (mRNA) localization facilitates efficient translation in cells such as neurons and fibroblasts. However, the extent and importance of mRNA polarization in epithelial tissues are unclear. Here, we used single-molecule transcript imaging and subcellular transcriptomics to uncover global apical-basal intracellular polarization of mRNA in the mouse intestinal epithelium. The localization of mRNAs did not generally overlap protein localization. Instead, ribosomes were more abundant on the apical sides, and apical transcripts were consequently more efficiently translated. Refeeding of fasted mice elicited a basal-to-apical shift in polarization of mRNAs encoding ribosomal proteins, which was associated with a specific boost in their translation. This led to increased protein production, required for efficient nutrient absorption. These findings reveal a posttranscriptional regulatory mechanism involving dynamic polarization of mRNA and polarized translation.

Intracellular mRNA localization is an important determinant of various cellular functions (1–6). In mammals, localized translation of transcripts at the sites where their encoded proteins are needed is thought to confer cellular efficiency and a timely response (2, 7, 8). Epithelial tissues are inherently polarized with distinct functional specialization of basal and apical sides. The intestinal epithelium consists

of a monolayer of enterocytes that absorb nutrients from the apical lumen and excrete them into the blood stream from the basal sides. Key transporters are specifically localized in these two compartments (9). Owing to the transient nature of nutrients in the gut, efficient and timely translation of such proteins might be important. The mRNA intracellular localization of a few enterocyte genes have been reported (10–12);

however, we lack a global characterization of intracellular mRNA localization and its biological functions in epithelia.

To obtain a transcriptome-wide view of mRNA localization in the intestinal epithelium, we isolated apical and basal subcellular fractions by laser capture microdissection (Fig. 1A) and performed RNA sequencing (RNA-seq) (13). Almost 30% of the most highly expressed 2000 transcripts, for which experimental noise levels were lower, were significantly polarized (Fig. 1B and table S1). To validate the sequencing results, we performed single-molecule fluorescence in situ hybridization (smFISH) (14) on intact intestinal tissues for 14 genes that span different polarization patterns (Fig. 1, B to D). We found an excellent correspondence between the apical bias of mRNA measured with smFISH and with the whole-transcriptome method (Spearman's $r = 0.97$, $P < 2.2 \times 10^{-16}$, Fig. 1D and table S2).

Given the functional polarization of enterocytes, we hypothesized that the observed global mRNA apical-basal polarization would match the location of the corresponding proteins. The most apically enriched gene sets included several nutrient transporter annotations, many of which encode apically localized proteins (fig. S1). Notably, however, the mRNAs that encode basolaterally localized proteins were strongly biased in localization toward the apical side, opposite to where their

¹Department of Molecular Cell Biology, Weizmann Institute of Science, Rehovot, Israel. ²Department of Molecular Genetics, Weizmann Institute of Science, Rehovot, Israel. ³Life Sciences Core Facilities, Weizmann Institute of Science, Rehovot, Israel.

*Corresponding author. Email: shalev.itzkovitz@weizmann.ac.il

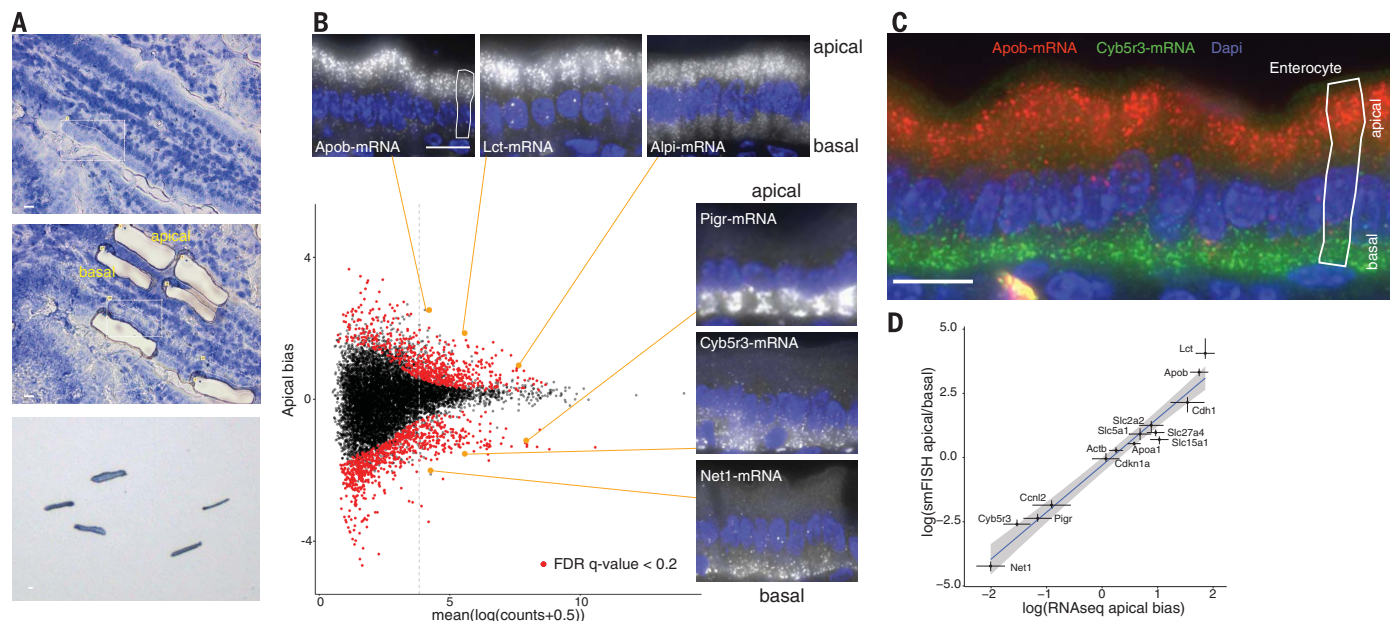


Fig. 1. Global analysis of mRNA polarization in the intestinal epithelium.

(A) Laser capture microdissection of paired apical and basal fragments. (B) RNA-seq data of isolated subcellular areas. Insets show smFISH validation results of transcripts of interest. Four outlier data points are omitted from the plot. Of the transcripts, 645 of 9905 are significantly apical and 779 of 9905 are significantly basal. Dashed vertical line separates the 2000 most highly

expressed transcripts, of which 392 genes are significantly apical and 194 are significantly basal. (C) smFISH staining of the apical Apob (red) and basal Cyb5r3 (green) mRNA. (D) Strong correlation of smFISH quantifications and RNAseq data for 14 representative genes (Spearman's $r = 0.97$, $P < 2.2 \times 10^{-16}$); dots and error bars represent median and 95% confidence interval of smFISH and mean and SE of RNAseq. All scale bars are 10 μ m.

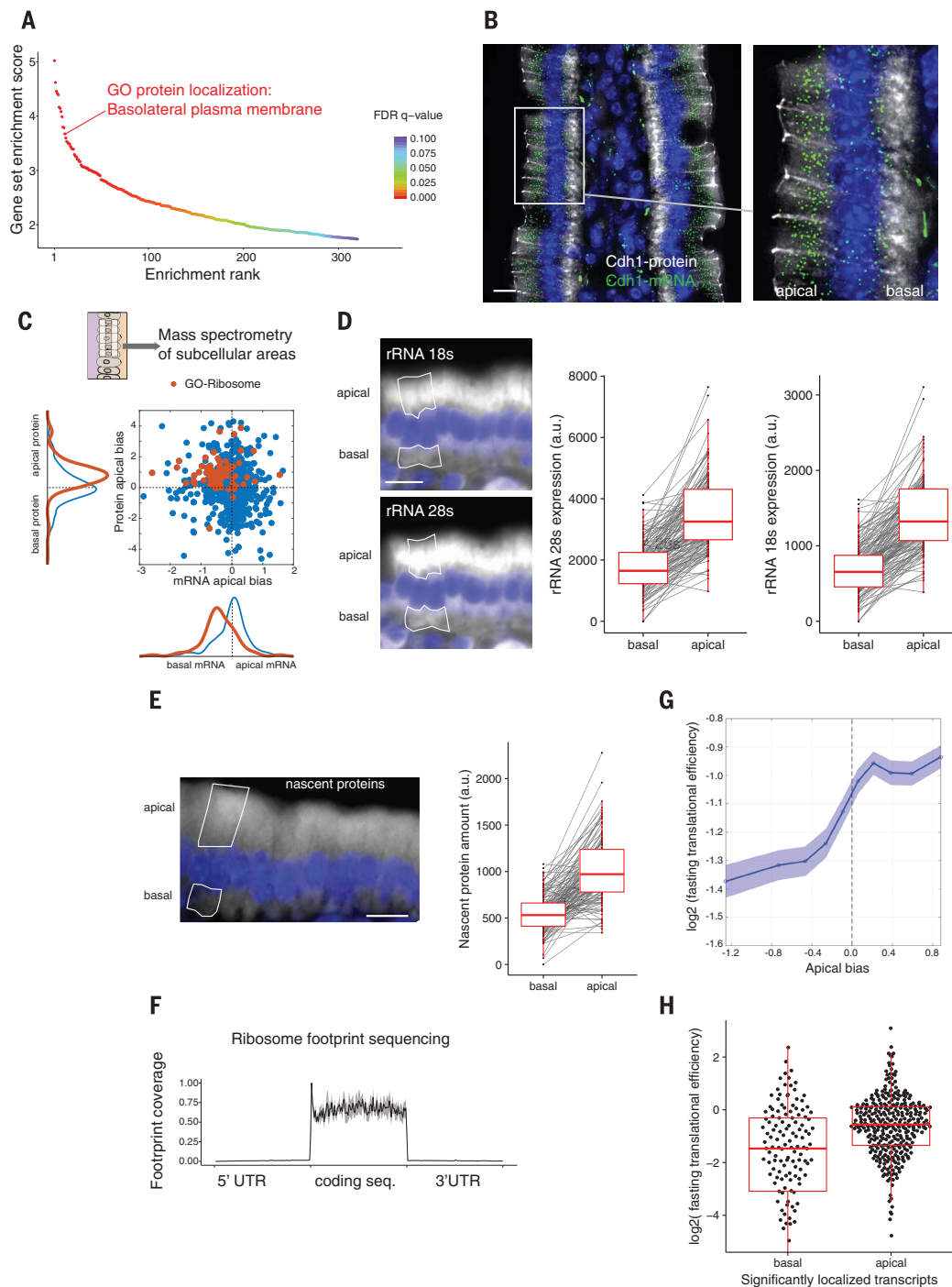


Fig. 2. Translational machinery is asymmetrically distributed.

(A) Ranking of gene sets that are significantly enriched on the apical cell sides. (B) Costaining of the discordantly localized basolateral protein E-cadherin, encoded by *Cdh1* (gray staining) and its apically localized mRNA (green dots).

(C) Mass spectrometry results of microdissected areas demonstrate apical enrichment of ribosomal proteins and a lack of positive correlation (Spearman's $r = -0.12$, $P = 8 \times 10^{-4}$). Blue, all genes; red, genes with GO-Ribosome annotation.

(D) Representative smFISH staining and quantification of intracellular distribution of rRNA 18S and 28S ($n = 142$ single cells, $P < 2.2 \times 10^{-16}$).

(E) Representative staining and quantification of nascent proteins ($n = 143$ single cells, $P < 2.2 \times 10^{-16}$).

(F) Normalized coverage plot of ribosome footprint sequencing data ($n = 3$ mice, gray area denotes SD).

(G) TE increases with the apical bias of genes in fasting mouse samples. The y axis shows the mean TE over a sliding window of 1000 genes consecutively shifted from the most basal gene to the most apical gene, with a 500-gene overlap. The x axis is the mean apical bias of genes within each window. Patches are standard errors of the mean.

(H) Translational efficiency of the significantly localized transcripts (false discovery rate adjusted P value < 0.1 , n apical = 346, n basal = 141, $P = 8.4 \times 10^{-10}$, 20 outlier data points are omitted from the plot). Data include only genes for which we obtained TE values and that are of epithelial origin (methods). All scale bars are 10 μ m.

encoded proteins reside (Fig. 2, A and B, and fig. S2A). Examples of basolateral proteins with discordantly polarized apical mRNA included E-cadherin (*Cdh1* gene, Fig. 2B) and integrins (fig. S2A). Thus, the global mRNA polarization in the intestinal epithelium does not generally correlate with the localization of the encoded proteins.

To obtain a broader view of the relative localization of mRNAs and their encoded proteins, we performed mass spectrometry of laser capture microdissected apical and basal subcellular fractions (Fig. 2C and table S3). The apical bias of proteins and of mRNA was weakly anticorrelated

(Spearman's $r = -0.12$, $P = 8 \times 10^{-4}$). This data set revealed additional examples of discordant localizations of proteins and their encoding mRNA, such as the basal protein sodium-potassium ATPase (adenosine triphosphatase), encoded by the highly apical mRNA *Atp1b1* (fig. S2A). Notably, the mass spectrometry data revealed a significantly higher abundance of ribosomal proteins at the apical side (Fig. 2C and table S4) and mitochondrial proteins at the basal sides (fig. S3 and table S4). The mRNAs that encode ribosomal proteins were basally biased, again constituting a discordant set of genes, with opposite localizations of mRNA and their en-

coded proteins (Fig. 2C). Using smFISH, we identified a highly significant apical enrichment of ribosomal RNA 18S and 28S (Fig. 2D and fig. S2B, both twofold, $P < 2.2 \times 10^{-16}$), thus validating the apically polarized localization of the translational machinery. To assess whether the increased concentration of ribosomes on the apical sides yields higher translation at this subcellular compartment, we treated mice with *O*-propargyl-puromycin (OPP), a reporter that is efficiently incorporated into nascent peptides after a pulse-chase intraperitoneal injection (15) (fig. S4). Nascent peptides were significantly more abundant on the apical

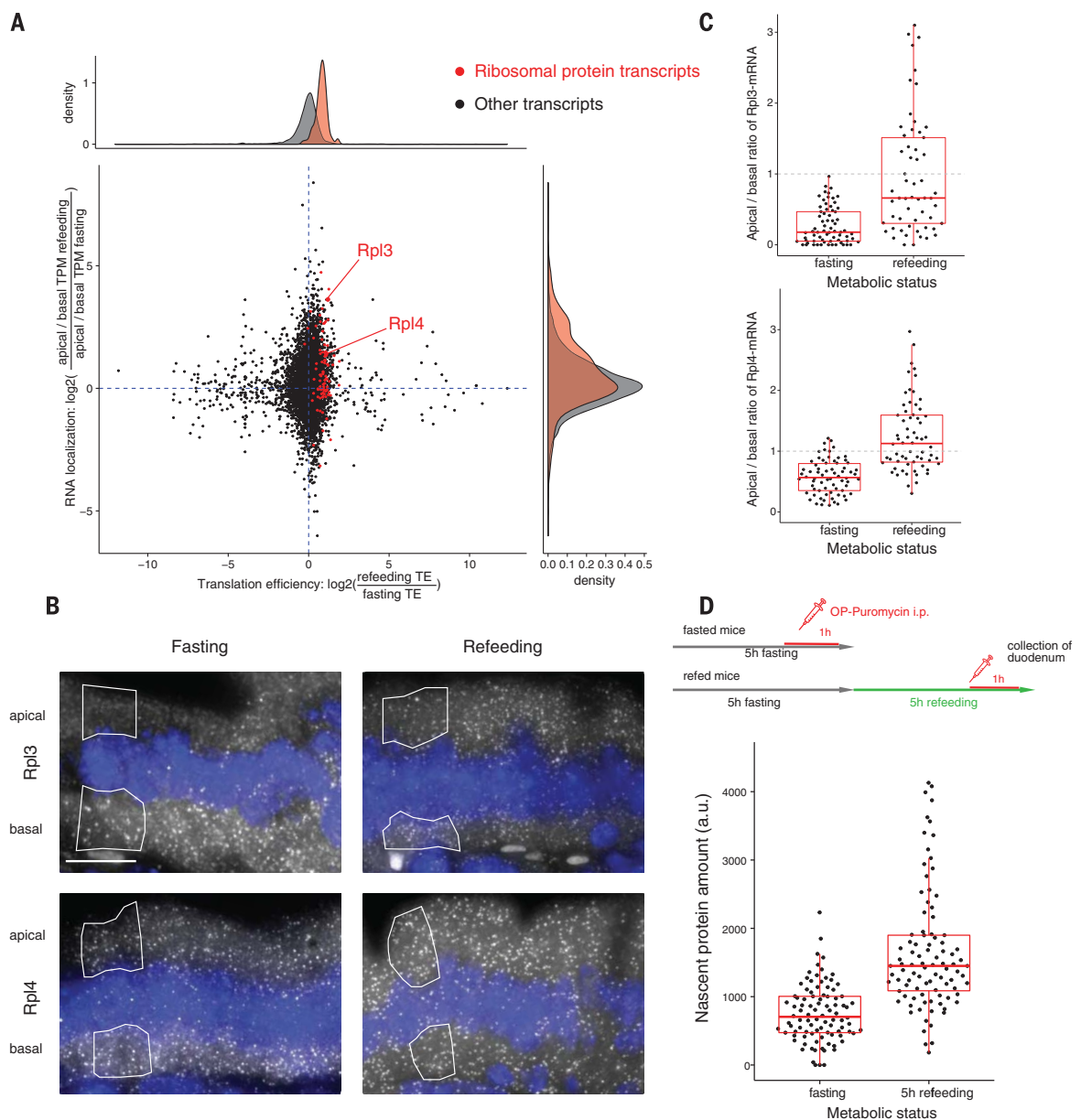
Fig. 3. Dynamic shifts of localized transcripts are associated with differential translational efficiency.

(A) Scatterplot of TE and mRNA localization changes when comparing three fasting and three refeed mice ($n = 6282$ transcripts). The x axis is \log_2 of the ratios between TEs in refeed and in fasting states; the y axis is \log_2 of the ratios of apical biases between refeed and fasting states, where apical bias for each condition is the ratio of apical and basal TPM (methods).

Upon refeeding, mRNAs encoding ribosomal proteins (red dots) become more apically polarized and are translated more efficiently. (B) smFISH images of Rpl3 and Rpl4 mRNA across metabolic states.

(C) Quantification of Rpl3 and Rpl4 smFISH analyses across metabolic states ($n = 70$ single cells, Rpl3 $P = 1.8 \times 10^{-8}$, Rpl4 $P = 2.9 \times 10^{-13}$).

(D) Comparison of nascent protein content at fasting and 5-hour refeeding time point ($n = 188$ single cells, $P < 2.2 \times 10^{-16}$). All scale bars are 10 μm .



sides of the intestinal enterocytes (Fig. 2E, 1.82-fold higher concentration at the apical side, $P < 2.2 \times 10^{-16}$). Thus, translation in the intestinal enterocytes is also strongly polarized, with a two-fold higher apical concentration of the translational machinery.

We next asked whether apical-basal mRNA polarization could regulate translation efficiency (TE) in this tissue. We performed ribosome profiling and RNA-seq of intestinal isolates from fasting mice and computed the TE of intestinal transcripts (Fig. 2F, fig. S5, and tables S5 and S6). Genes with significantly apical mRNA localization had almost twofold higher TE compared to genes with significantly basal mRNA (Fig. 2, G and H, $P = 8.36 \times 10^{-10}$). In several nonpolarized mouse primary cell data sets, the apical and basal groups were either indistinguishable or dis-

played much weaker apical enrichment of TE (fig. S6A). Thus, mRNA apico-basal polarization modulates TE in the intestinal epithelium.

The intestinal lumen is a highly dynamic microenvironment that exhibits temporal oscillation in nutrient availability (16). Dynamic translocation of mRNA between the basal and apical sides could potentially modulate translational efficiency. To explore such dynamic responses, we performed our transcriptome-wide mRNA polarization measurements and ribosome profiling on duodenum tissues of fasting and refeed mice (Fig. 3A). The translational machinery remained apical after refeeding, as evident by the apical polarization of ribosomal RNA (rRNA) (fig. S6B), and the TE of genes was higher the more apically polarized were their transcripts (fig. S6C). mRNAs that encode ribosomal proteins (RNA-RPs) shifted from the

basal localization in fasted intestines to a more apical localization after 2 hours of refeeding (Fig. 3A, 1.36-fold for RNA-RPs versus 1.08-fold for other transcripts, $P = 0.0001$). We also observed a concomitant increase in TE for these transcripts upon shifting their localization to the apical side—the side in which the translation machinery is more abundant (Fig. 3A and fig. S7, 1.87-fold, $P < 2 \times 10^{-16}$). We validated these localization changes for Rpl3 and Rpl4 mRNA by smFISH (Fig. 3, B and C, Rpl3 $P = 1.8 \times 10^{-8}$, Rpl4 $P = 2.9 \times 10^{-13}$). The cellular mRNA expression levels of these genes were not increased (fig. S8, A to C). After 4 hours of refeeding, increased production of ribosomal components was associated with significantly higher protein synthesis compared to the fasting state (Fig. 3D, 2.05-fold, $P < 2.2 \times 10^{-16}$). TE of brush border proteins (17) also showed a slight,

Fig. 4. Intestinal mRNA localization is mediated by the microtubule network.

(A) Nocodazole strongly perturbs the polarization of Net1 and Apob (Net1 $n = 94$ cells, $P = 1.1 \times 10^{-15}$, Apob $n = 96$ cells, $P = 2.9 \times 10^{-12}$).

(B) Representative smFISH images of strongly polar Net1 and Apob transcripts in vehicle- or nocodazole-injected animals. Scale bar, 10 μm . **(C)** Intracellular mRNA localization of Net1 and Apob in intestinal organoids phenocopies in vivo observations. Highlighted inset is shown in higher magnification in top row of (D). Scale bar, 50 μm .

(D) smFISH images of Net1 and Apob in nocodazole-, isipinesib-, or vehicle-treated organoids. Scale bar, 10 μm .

(E) Single-cell quantification of the nocodazole and isipinesib effects on transcript localization in smFISH images of intestinal organoids (vehicle $n = 101$, isipinesib $n = 68$, nocodazole $n = 77$ cells, costaining of Apob and Net1).

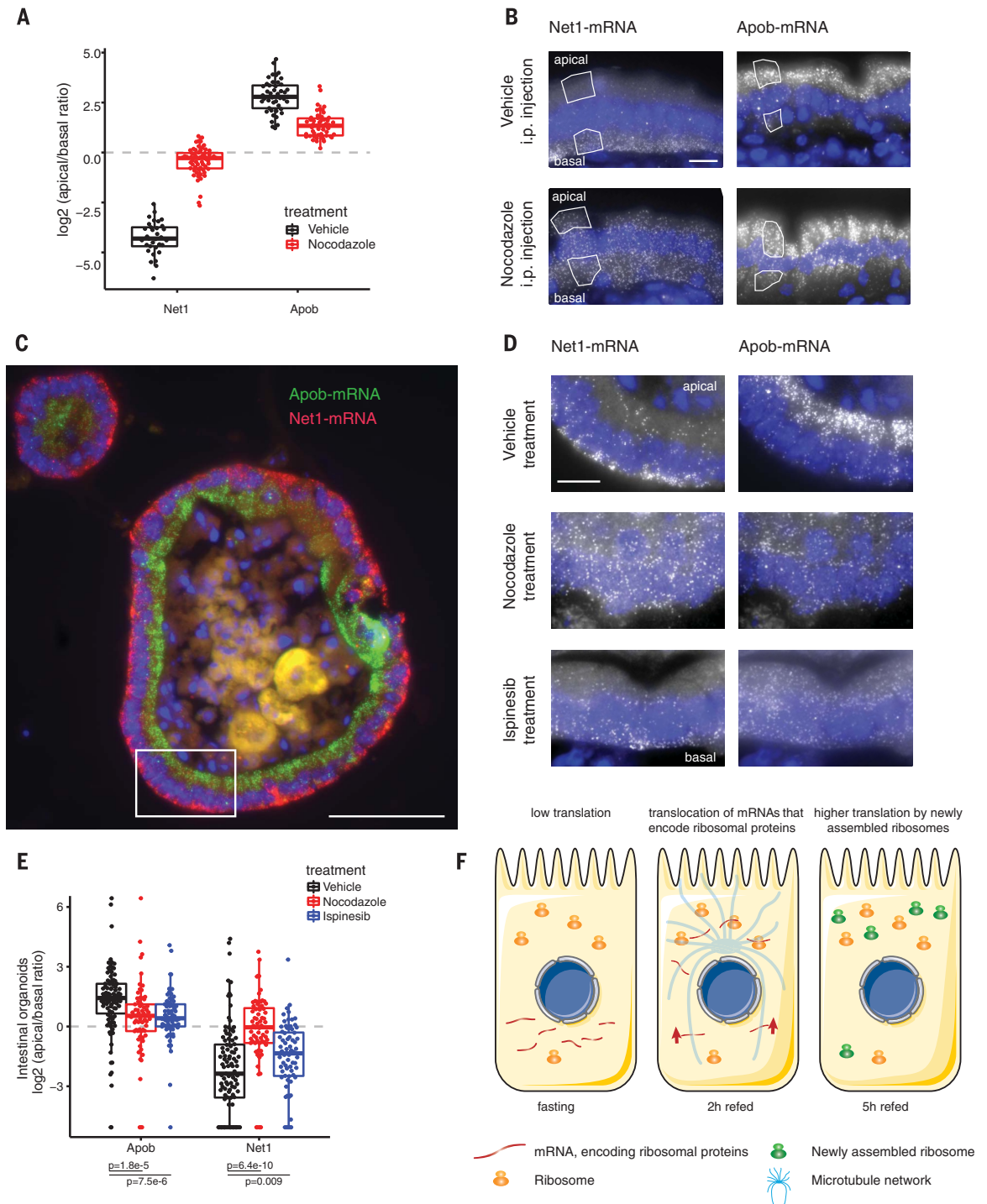
(F) Transcripts that encode ribosomal proteins are stored in the less translationally active basal side of the intestinal epithelium in fasting mice. Refeeding induces a translocation of these transcripts into the more translationally active apical cell side. This translocation is associated with a concomitant increase in their translational efficiency. The increased ribosomal biogenesis is reflected in an increased total protein synthesis.

yet significant increase upon refeeding (1.1-fold, $P = 0.02$, fig. S8D). Thus, dynamic translocation of mRNAs encoding ribosomal proteins to the more translationally active apical side is associated with a specific translation of ribosomal components, facilitating a burst of protein production to meet the absorption demands upon refeeding.

What facilitates this broad mRNA polarization? Active transport by motor proteins along the

cytoskeleton, molecular anchors that bind and keep transcripts localized, or spatially varying RNA degradation rates within the cell have all been implicated in determining localization (1, 18). Additionally, our finding that the ribosomes are apically polarized in enterocytes could indicate that preferential retention of highly translated mRNA could lead to their apical polarization (1, 18). To investigate whether microtubules me-

diate the observed mRNA localization patterns, we depolymerized the microtubule network by injecting mice intraperitoneally with nocodazole (Fig. 4, A and B). The basally polarized Net1, Cyb5r3, Rpl3, and Rpl4 transcripts lost polarization, and the apically polarized Apob and Cdh17 transcripts were significantly less apical (Fig. 4, A and B, and fig. S9). Although ribosomal RNA remained significantly apically polarized in



nocodazole-treated mice, the extent of rRNA polarization was smaller compared to that in vehicle-treated controls (fig. S10). To assess whether the difference in polarization of apical mRNA upon nocodazole treatment could stem from coordinated movement of ribosomes and their retained mRNA to the basal side, we measured the combined polarization of both rRNA and of four apical genes with high TE in nocodazole-treated mice and in controls, and stratified the results according to the single-cell rRNA polarization. Microtubule disruption decreased the apical polarization of these genes even when controlling for rRNA polarization changes (figs. S10 and S11A). Thus, the microtubule network mediates the asymmetric localization of these and potentially other transcripts in the intestinal epithelium, whereas additional anchoring mechanisms seem to render the apical localization of ribosomes less sensitive to microtubule disruption. Selective inhibition of kinesin 5 in intestinal organoids (19, 20) using *ispinesib* (21) decreased the polarization of *ApoB* and *Net1* (Fig. 4, C to E) but not of *Cdh17* and *Pigr* (fig. S9, E and F).

Given the transient nature of inputs in the gut, consistently high translation rates could be energetically inefficient (22). When nutrients arrive, however, there is a short temporal window in which they must be efficiently absorbed (9). Nutrient availability was shown to stimulate rapid ribosome biogenesis in other contexts (23, 24) via activation of translation initiation factors, rRNA transcription, and translation of RNAs that encode the translational machinery (24). Here, we found a similar burst of protein translation upon refeeding, associated with a rapid translocation of ribosomal-protein encoding transcripts, the nature of which is yet to be determined, into the translationally active apical

side (Fig. 4F). The burst of ribosomal protein translation upon refeeding resembles a “bang-bang” control strategy, in which resources are first invested in making the ribosomal “machines,” to facilitate a rapid increase in total protein output (25, 26). Our approach, combining laser-capture microdissection and whole-transcriptome sequencing with smFISH, can be readily applied to characterize mRNA polarization in other tissues and organisms. Future studies will determine if mRNA mislocalizations are causatively involved in pathophysiology.

REFERENCES AND NOTES

1. A. R. Buxbaum, G. Haimovich, R. H. Singer, *Nat. Rev. Mol. Cell Biol.* **16**, 95–109 (2015).
2. C. E. Holt, S. L. Bullock, *Science* **326**, 1212–1216 (2009).
3. K. C. Martin, A. Ephrussi, *Cell* **136**, 719–730 (2009).
4. E. Lécuyer *et al.*, *Cell* **131**, 174–187 (2007).
5. S. Mill, K. Moissoglu, I. G. Macara, *Nature* **453**, 115–119 (2008).
6. H. Jambor *et al.*, *eLife* **4**, e05003 (2015).
7. F. Besse, A. Ephrussi, *Nat. Rev. Mol. Cell Biol.* **9**, 971–980 (2008).
8. A. J. Rodriguez, K. Czaplinski, J. S. Condeelis, R. H. Singer, *Curr. Opin. Cell Biol.* **20**, 144–149 (2008).
9. K. N. Frayn, *Metabolic Regulation: A Human Perspective* (Wiley-Blackwell, Chichester, UK, ed. 3, 2010).
10. E. H. H. M. Rings *et al.*, *FEBS Lett.* **300**, 183–187 (1992).
11. J. A. Barth *et al.*, *J. Histochem. Cytochem.* **46**, 335–343 (1998).
12. W. Li, S. D. Krasinski, M. Verhave, R. K. Montgomery, R. J. Grand, *Gastroenterology* **115**, 86–92 (1998).
13. S. Nichterwitz *et al.*, *Nat. Commun.* **7**, 12139 (2016).
14. A. Raji, P. van den Bogaard, S. A. Rifkin, A. van Oudenaarden, S. Tyagi, *Nat. Methods* **5**, 877–879 (2008).
15. J. Liu, Y. Xu, D. Stoleru, A. Salic, *Proc. Natl. Acad. Sci. U.S.A.* **109**, 413–418 (2012).
16. C. A. Thaiss *et al.*, *Cell* **167**, 1495–1510.e12 (2016).
17. R. E. McConnell, A. E. Benesh, S. Mao, D. L. Tabb, M. J. Tyska, *Am. J. Physiol. Gastrointest. Liver Physiol.* **300**, G914–G926 (2011).
18. C. A. Pratt, K. L. Mowry, *Curr. Opin. Cell Biol.* **25**, 99–106 (2013).
19. T. Sato *et al.*, *Nature* **459**, 262–265 (2009).
20. T. Sato *et al.*, *Gastroenterology* **141**, 1762–1772 (2011).
21. L. Lad *et al.*, *Biochemistry* **47**, 3576–3585 (2008).
22. D. F. Rolfe, G. C. Brown, *Physiol. Rev.* **77**, 731–758 (1997).
23. C. Mayer, I. Grummt, *Oncogene* **25**, 6384–6391 (2006).
24. M. Laplante, D. M. Sabatini, *Cell* **149**, 274–293 (2012).
25. S. Itzkovitz, I. C. Blat, T. Jacks, H. Clevers, A. van Oudenaarden, *Cell* **148**, 608–619 (2012).
26. D. Madar *et al.*, *BMC Syst. Biol.* **7**, 136 (2013).

ACKNOWLEDGMENTS

We thank K. Bahar Halpern, B. Toth, and S. Ben-Moshe for valuable comments on the manuscript. We thank the L. Lokey animal facility (Weizmann Institute of Science, Rehovot, Israel), the Crown Institute for Genomics (Weizmann Institute of Science, Rehovot, Israel), and the Smoler Protein Research Center (Technion, Haifa, Israel) for help with experimental procedures. A.E.M. is supported by the Swiss National Science Foundation (grant 158999) and the European Molecular Biology Organization (EMBO) Long-Term Fellowship program (ALTF 306-2016). N.S.-G. research is funded by the European Research Council starting grant (StG-2014-638142). N.S.-G. is incumbent of the Skirball Career Development Chair in New Scientists. S.I. is supported by the Henry Chanoch Kreter Institute for Biomedical Imaging and Genomics, The Leir Charitable Foundations, Richard Jakubskind Laboratory of Systems Biology, Cymerman-Jakubskind Prize, The Lord Sieff of Brimpton Memorial Fund, the I-CORE program of the Planning and Budgeting Committee and the Israel Science Foundation (grants 1902/12 and 1796/12), the Israel Science Foundation grant no. 1486/16, the EMBO Young Investigator Program, and the European Research Council under the European Union’s Seventh Framework Programme (FP7/2007-2013)–ERC grant agreement no. 335122. S.I. is the incumbent of the Philip Harris and Gerald Ronson Career Development Chair. All data supporting the findings of this study and all analysis codes are available within the article and its supplementary materials or from the corresponding author upon request. The generated sequencing data have been deposited in the GenBank Gene Expression Omnibus database (www.ncbi.nlm.nih.gov/geo/) under accession code GSE95416.

SUPPLEMENTARY MATERIALS

www.sciencemag.org/content/357/6357/1299/suppl/DC1
Materials and Methods
Figs. S1 to S11
Tables S1 to S7
References (27–52)

16 March 2017; resubmitted 3 July 2017
Accepted 1 August 2017
Published online 10 August 2017
10.1126/science.aan2399

Global mRNA polarization regulates translation efficiency in the intestinal epithelium

Andreas E. Moor, Matan Golan, Efi E. Massasa, Doron Lemze, Tomer Weizman, Rom Shenhav, Shaked Baydatch, Orel Mizrahi, Roni Winkler, Ofra Golani, Noam Stern-Ginossar and Shalev Itzkovitz

Science **357** (6357), 1299-1303.

DOI: 10.1126/science.aan2399originally published online August 10, 2017

Location, location, location

The distribution of RNA in cells is important for efficient translation into proteins. Asymmetric RNA localization is known in several cell types but is poorly understood in gut epithelial cells. Moor *et al.* found that transcripts in intestinal enterocytes tend to distribute to the cells' apical or basal cell sides (see the Perspective by Gáspár and Ephrussi). mRNA localization does not generally overlap protein localization; instead, ribosomes are apically biased, which allows more efficient translation. On refeeding of fasted mice, gut cell mRNAs encoding ribosomal proteins exhibit a basal-to-apical shift in localization and a boost in translation. Thus, dynamic polarization of mRNA and polarized translation modulate translational efficiency in the intestinal epithelium.

Science, this issue p. 1299; see also p. 1235

ARTICLE TOOLS

<http://science.sciencemag.org/content/357/6357/1299>

SUPPLEMENTARY MATERIALS

<http://science.sciencemag.org/content/suppl/2017/08/09/science.aan2399.DC1>

RELATED CONTENT

<http://science.sciencemag.org/content/sci/357/6357/1235.full>

REFERENCES

This article cites 51 articles, 9 of which you can access for free
<http://science.sciencemag.org/content/357/6357/1299#BIBL>

PERMISSIONS

<http://www.sciencemag.org/help/reprints-and-permissions>

Use of this article is subject to the [Terms of Service](#)